Natural drinking strategies

Wonjung Kim and John W. M. Bush

Journal of Fluid Mechanics / Volume 705 / August 2012, pp 7 - 25
DOI: 10.1017/jfm.2012.122, Published online: 17 April 2012

J. Fluid Mech. (2012), *vol.* 705, *pp.* 7–25.
doi:10.1017/jfm.2012.122

Natural drinking strategies

Wonjung Kim[1] **and John W. M. Bush**[2]†

[1] Department of Mechanical Engineering, Massachusetts Institute of Technology, 77 Massachusetts Avenue, Cambridge, MA 02139, USA

[2] Department of Mathematics, Massachusetts Institute of Technology, 77 Massachusetts Avenue, Cambridge, MA 02139, USA

(Received 30 May 2011; revised 17 November 2011; accepted 27 February 2012; first published online 17 April 2012)

We examine the fluid mechanics of drinking in nature. We classify the drinking strategies of a broad range of creatures according to the principal forces involved, and present physical pictures for each style. Simple scaling arguments are developed and tested against existing data. While suction is the most common drinking strategy, various alternative styles have evolved among creatures whose morphological, physiological and environmental constraints preclude it. Particular attention is given to creatures small relative to the capillary length, whose drinking styles rely on relatively subtle interfacial effects. We also discuss attempts to rationalize various drinking strategies through consideration of constrained optimization problems. Some biomimetic applications are discussed.

Key words: flow–vessel interactions, micro-organism dynamics, peristaltic pumping

1. Introduction

Sir James Lighthill coined the word ‘biofluiddynamics’ to describe fluid mechanics problems arising in biology (Lighthill 1975), a theme that has been pursued with great success by the honouree of this edition. Substantial effort has been devoted to elucidating natural locomotion strategies, including those of fish (Triantafyllou, Triantafyllou & Yue 2000), flying insects (Wang 2005), birds (Wu 2011) and micro-organisms (Pedley & Kessler 1992; Lauga & Powers 2009). Flow through elastic tubes has been examined in order to elucidate the dynamics of flows in the respiratory, pulmonary (Pedley 1977) and nervous systems (Carpenter, Berkouk & Lucey 2003). ‘Biocapillarity’ might likewise be used to describe the subset of biofluiddynamics problems dominated by interfacial effects. One well-explored such problem is that of natural strategies for water repellence employed by plants and insects (Bush, Hu & Prakash 2008), which have served as a source of inspiration in the design of superhydrophobic surfaces (Carré & Mittal 2009). Another is the role of surfactants in the respiratory system, a problem of critical importance in the treatment of premature infants (Grotberg 1994). More recently, natural strategies for propulsion at the water surface have been explored (Bush & Hu 2006). Here we examine natural strategies for fluid transport, wherein a number of novel biocapillary problems arise.

† Email address for correspondence: bush@math.mit.edu

Although water can be ingested with food, drinking is the principal route for water intake, critical in the sustenance of most animals. We loosely define drinking as fluid uptake required for the sustenance of life. Some creatures uptake water in order to capture suspended prey; for example, flamingoes feed on algae suspended in water (Zweers *et al.* 1995), and tiger salamanders capture aquatic prey by drawing in water (Gillis & Lauder 1994). Finally, we note that drinking need not involve water; for example, many insects and birds ingest fluid primarily in the form of nectar, which serves also as their principal source of energy. Nectar drinking will be one subject of focus in our study.

Most creatures ingest fluid either by suction through an orifice (e.g. lips or a beak) or a tube (e.g. a proboscis or a trunk) or by entrainment onto the tongue. However, drinking styles in nature are myriad, depending on the creature's size, the morphology of its mouth parts and its environment. Some creatures have developed ingenious drinking techniques in response to harsh environmental constraints. In most previous studies of drinking strategies, emphasis was given to reporting observations of particular drinking styles. Only in very few such studies have the fluid mechanics of drinking been highlighted. Dynamic models for nectar drinking in hummingbirds and butterflies were established by Kingsolver & Daniel (1983) and Pivnick & McNeil (1985). In an attempt to rationalize observed drinking rates for butterflies, Kingsolver & Daniel (1979) were the first to pose nectar drinking through a tube as a constrained optimization problem, an approach that has recently been advanced by Kim, Gilet & Bush (2011). Prakash, Quéré & Bush (2008) demonstrated that a class of shorebirds relies on contact angle hysteresis for the mouthward transport of prey-bearing droplets. Recently, Reis *et al.* (2010) and Crompton & Musinsky (2011) rationalized the drinking strategies of cats and dogs, respectively, demonstrating that they use inertial forces generated by their lapping tongues to overcome gravity.

In the current study, we focus on terrestrial creatures, excluding from consideration underwater creatures, such as fish and amphibians, that drink primarily via osmosis. In § 2, we categorize the drinking styles of a broad range of terrestrial creatures by identifying the principal force balances involved in the fluid transport. We suggest consistent physical pictures and present simple scalings that describe the dynamics of each drinking style, specifically suction (§ 3), dipping, licking (§ 4), lapping and ladling (§ 5). Finally, several novel drinking techniques that rely on contact angle hysteresis are highlighted in § 6.

2. Dynamic classification

The drinking styles of terrestrial creatures, as shown in figure 1, can be classified according to the dominant driving and resistive forces. Drinking is generally accomplished by virtue of a driving pressure generated by some combination of muscular contraction and capillarity, and resisted by some combination of fluid inertia, gravity and viscosity. The dominant driving and resisting forces depend on the size and morphology of drinkers as well as the properties of the fluid.

Consider a fluid of density ρ and viscosity μ being driven with velocity u through a domain of characteristic scale L by a pressure difference ΔP in the presence of a gravitational acceleration g. Characteristic magnitudes of the various hydrodynamic forces may be written as $F_{inertia} \sim \rho u^2 L^2$, $F_{viscous} \sim \mu u L$, $F_{pressure} \sim \Delta P L^2$ and $F_{gravitational} \sim \rho g L^3$. In drinking, ΔP is typically produced by either muscular contraction or interfacial curvature. In the latter case, it scales as $\Delta P \sim \sigma/L$, where σ is the surface tension. The relative magnitudes of the various force components

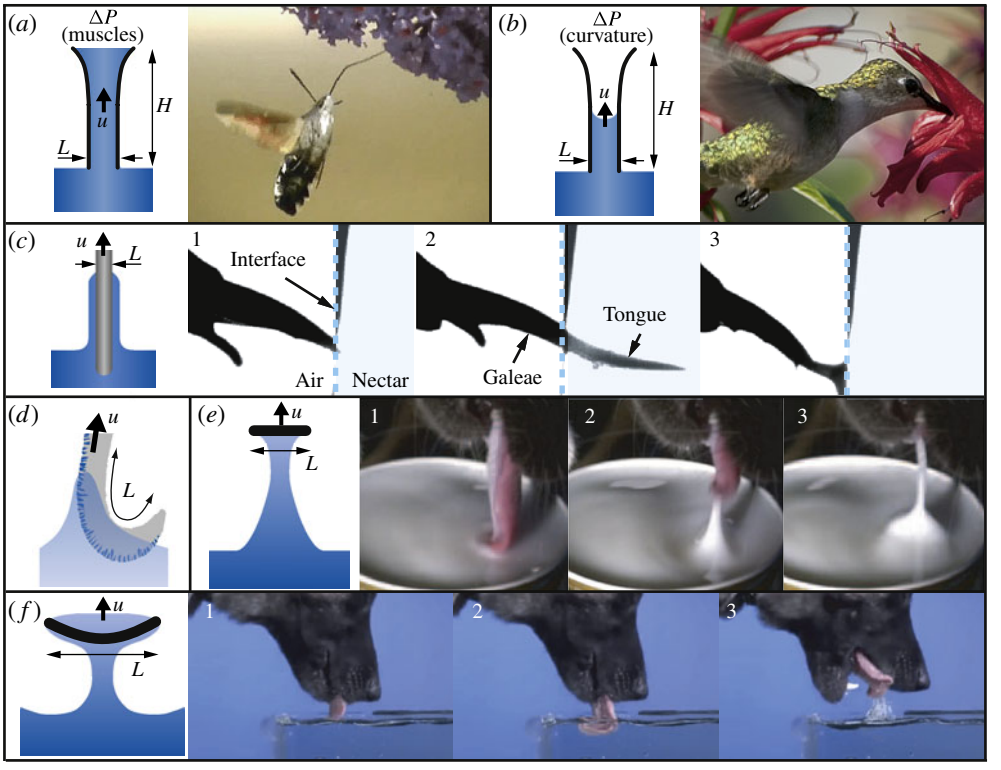

FIGURE 1. (Colour online available at journals.cambridge.org/flm) Various drinking techniques. Schematic illustration of (*a*) viscous suction, as employed by a moth; (*b*) capillary suction, as employed by a hummingbird; (*c*) viscous dipping, as employed by a bee (Kim *et al.* 2011); (*d*) licking, as employed by a lizard; (*e*) lapping, as employed by a cat (Reis *et al.* 2010); and (*f*) ladling, as employed by a dog. Images courtesy of (*a*) Small Wildlife Films, (*b*) Richard Houde, (*e*) Pedro Reis, and (*f*) Discovery Networks (http://dsc.discovery.com/videos/time-warp-dog-drinking-water.html).

can be written in terms of standard dimensionless groups, specifically the Reynolds number, $Re = \rho uL/\mu$ (denoting the ratio of inertial to viscous forces), the Bond number, $Bo = \rho gL^2/\sigma$ (the ratio of hydrostatic to capillary forces), and the capillary number, $Ca = \mu u/\sigma$ (the ratio of viscous to capillary forces).

Many creatures, including nectar-feeding or blood-sucking insects, use tubes (e.g. probosci, snouts or trunks) of high aspect ratio H/L, where H and L are the characteristic length and diameter of the tube, respectively. For such tube feeders, the inertial and viscous forces scale as $F_{inertia} \sim \rho u^2 L^2$ and $F_{viscous} \sim \mu uH$, so their relative magnitude is prescribed by the reduced Reynolds number, $\widetilde{Re} = Re(L/H)$. Moreover, $F_{gravitational} \sim \rho gHL^2$ and $F_{curvature} \sim \sigma L$, so their relative magnitude is prescribed by the reduced Bond number, $\widetilde{Bo} = Bo(H/L)$, where $Bo = \rho gL^2/\sigma$. Assessment of the magnitudes of these dimensionless groups indicates the dominant forces at play. The $\widetilde{Re}$ and $\widetilde{Bo}$ for various creatures are compiled in figure 2, where the different drinking styles are represented by different colours. For creatures that do not rely on tubes for drinking, $H \sim L$, so $\widetilde{Re} = Re$ and $\widetilde{Bo} = Bo$. We first discuss general characteristics

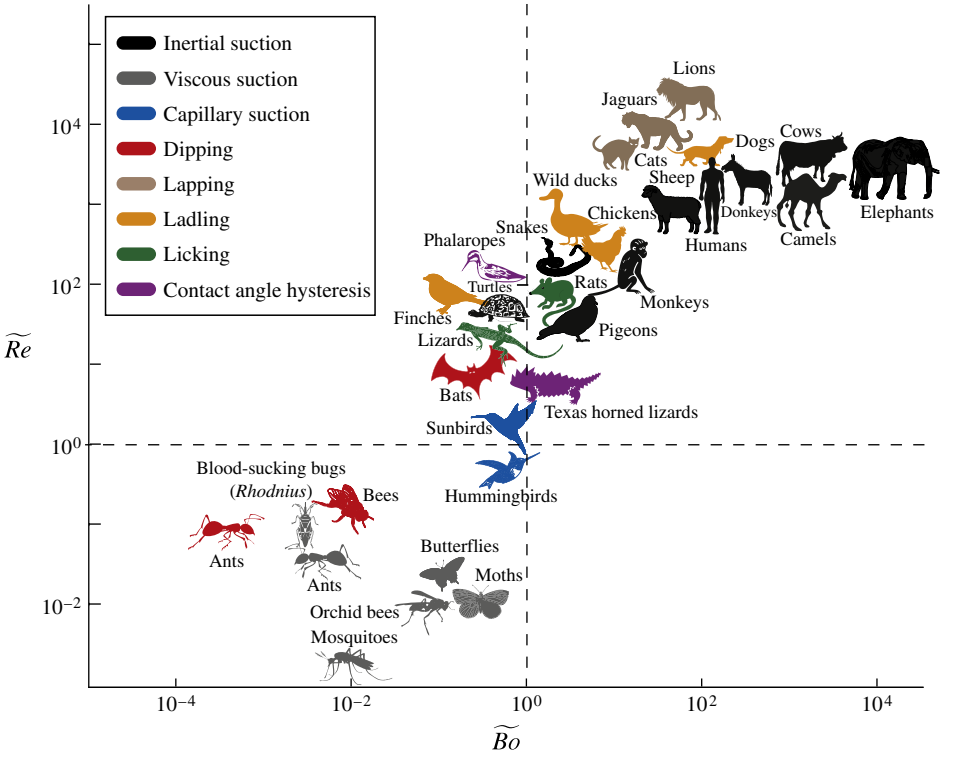

FIGURE 2. Drinking styles as a function of $\widetilde{Re} = (\rho u L/\mu)(L/H)$ and $\widetilde{Bo} = \rho g H L/\sigma$. For tube feeders, L and H are the tube diameter and height, respectively; for others, $L = H$ is the characteristic mouth size. Data are compiled from various sources: elephants (Wilson *et al.* 1991; West 2001), cows (Andersson, Schaar & Wiktorsson 1984), camels (Schmidt-Nielsen *et al.* 1956), lions (Reis *et al.* 2010), dogs (Adolph 1939), donkeys (Schmidt-Nielsen *et al.* 1956), jaguars (Reis *et al.* 2010), humans (Morrison *et al.* 1989), sheep (Bott, Denton & Weller 1965), cats (Reis *et al.* 2010), monkeys (Maddison *et al.* 1980), chickens (Heidweiller, van Loon & Zweers 1992), wild ducks (Kooloos & Zweers 1989), snakes (Berkhoudt, Kardong & Zweers 1995; Cundall 2000), rats (Weijnen 1998; McClung & Goldberg 2000), pigeons (Zweers 1982), finches (Heidweiller & Zweers 1990), phalaropes (Prakash *et al.* 2008), turtles (Bentley, Bretz & Schmidt-Nielsen 1967; Davenport & Macedo 1990; Bels, Davenport & Renous 1995), lizards (Wagemans *et al.* 1999), Texas horned lizards (Sherbrooke 2004), bats (Roces, Winter & von Helversen 1993; Winter & von Helversen 2003), sunbirds (Schlamowitz, Hainsworth & Wolf 1976), hummingbirds (Kingsolver & Daniel 1983; Tamm & Gass 1986), orchid bees (Borrell 2006, 2007), bees (Harder 1986), mosquitoes (Rosenson, McCormick & Uretz 1996; Lee, Kim & Lee 2009), moths (Josens & Farina 2001), butterflies (Pivnick & McNeil 1985), ants (Paul & Roces 2003) and *Rhodnius* (Bennet-Clark 1963).

of the drinking styles represented on the plot; later, we present a more technical examination.

For large creatures, including most mammals, $\widetilde{Bo} \gg 1$, so capillary pressures are negligible. Fluid transport is thus typically generated by pressure induced by muscular contraction, except in the case of a few creatures such as cats and dogs, which have morphological constraints that preclude suction (Reis *et al.* 2010). Reptiles, amphibians and birds, for which $\widetilde{Bo} \sim 1$, can exploit capillary forces and so exhibit a

relatively diverse variety of drinking styles. Small creatures such as insects, for which $\widetilde{Bo} \ll 1$ and $\widetilde{Re} \ll 1$, rely principally on some combination of capillary suction and viscous entrainment.

3. Suction

Suction is the most common drinking strategy in nature. We classify suction drinking styles according to what produces the driving pressure and whether the flow is resisted principally by fluid inertia or viscosity. The pressure-driven flow with mean speed u of a fluid of density ρ and viscosity μ along a tube of diameter d and height h is described by Newton's second law:

$$(m + m_a)\dot{u} = \frac{\pi}{4}d^2\Delta P - mg - \frac{\pi}{8}\rho u^2 d^2 - \pi h\, d\tau. \tag{3.1}$$

Here m is the mass of the fluid in the tube, m_a the added mass of the fluid preceding the inlet of the tube, ΔP the pressure difference applied at the height h of the fluid and τ the shear stress along the outer wall. One can estimate m, m_a and τ as

$$m = \frac{\pi}{4}\rho d^2 h, \quad m_a = k_1\frac{\pi}{4}\rho d^3, \quad \tau = k_2\mu\frac{u}{d}, \tag{3.2}$$

where k_1 and k_2 are order-one constants. After dividing by $\pi d^2/4$, rearrangement of (3.1) yields

$$\Delta P = \rho\left(1 + k_1\frac{d}{h}\right)h\dot{u} + \frac{1}{2}\left(1 + \frac{8k_2}{Re(d/h)}\right)\rho u^2 + \rho g h, \tag{3.3}$$

where $Re = \rho u d/\mu$. When fluid is accelerating, the characteristic acceleration time is of the order of h/u, so that $\dot{u} \sim u^2/h$. We further note that, while the shape of the mouth parts varies widely, commonly $d/h \leqslant 1$, particularly for tube feeders.

For active suction, ΔP is generated by muscular contraction, while for capillary suction, $\Delta P \sim \sigma/d$ is the Laplace or capillary pressure. A cornerstone of biomechanics is that the force that a creature of characteristic size l can generate is $F \sim l^2$ (McMahon & Bonner 1983); thus, one expects the suction pressure generated by muscles, $\Delta P \sim F/l^2 \sim l^0$, to be independent of scale and so to be of comparable magnitude for all creatures. For example, $\Delta P \sim 10$ kPa for mosquitoes (Lee *et al.* 2009), humans (Morrison *et al.* 1989) and elephants (West 2001); the highest ΔP appears to be 80 kPa for bed bugs (Daniel & Kingsolver 1983). We can thus infer the tube diameter $d \sim \sigma/\Delta P \sim 10$ μm below which capillary pressure dominates the applied suction pressure. For most creatures, the tube or mouth diameter d is significantly larger than 10 μm, so the capillary pressure is negligible. Nevertheless, capillary suction is employed by certain creatures for which applied suction is precluded by virtue of geometrical and physiological constraints, such as the open, passive tongue of the hummingbird (§ 3.3) (Kim *et al.* 2012) and the open beak of the zebra finch.

We can also use the near constancy of the suction pressure ΔP across species to assess the tube height $h \sim \Delta P/\rho g \sim 1$ m below which the applied suction pressure dominates hydrostatic pressure. For virtually all creatures using active suction (except the elephant), $h \ll 1$ m, indicating the relatively minor effect of gravity on the dynamics. Also, most capillary suction feeders have tubes of characteristic length $h \sim 1$ cm; consequently, $\rho g h d/\sigma \sim 0.1$ and the effect of gravity is negligible. In this

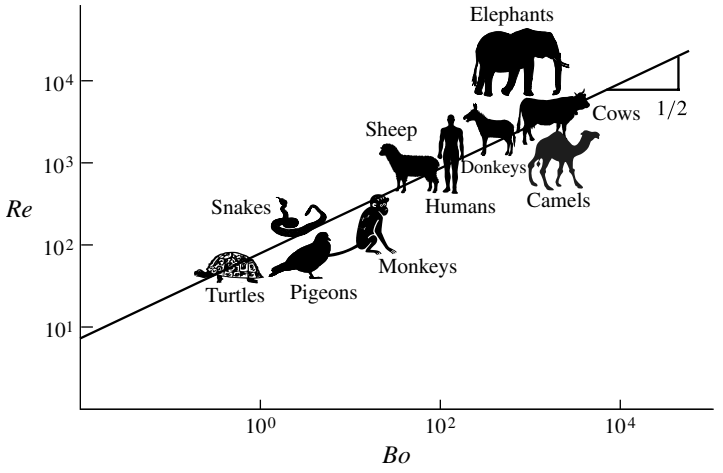

FIGURE 3. Plot of $Re = \rho u d/\mu$ against $Bo = \rho g d^2/\sigma$ for creatures employing inertial suction. We note that, since inertial suction does not depend on surface tension, Bo is here simply a proxy for body size.

limit, (3.3) may be expressed as

$$\Delta P \sim \left(\frac{3}{2} + \frac{4k_2}{Re(d/h)}\right)\rho u^2. \tag{3.4}$$

The applied suction pressure must overcome inertial and viscous resistance, the relative magnitudes of which are prescribed by $Re(d/h)$.

3.1. *Inertial suction* $(Re(h/d) \gg 1)$

For many large creatures, including humans, monkeys, sheep and pigeons, $Re(d/h) \gg 1$, and the fluid speed in (3.4) scales as $u \sim (\Delta P/\rho)^{1/2}$. Therefore, Re may be expressed as

$$Re = \frac{\rho u d}{\mu} \sim \left(Bo\frac{\sigma\,\Delta P}{\mu^2 g}\right)^{1/2}, \tag{3.5}$$

where $Bo = \rho g d^2/\sigma$. Assuming ΔP to be comparable for all suction drinkers, one expects a slope of $1/2$ in the plot of Re against Bo, as evident in figure 3. Scatter in the data presumably results from morphological variation between species. Specifically, $h \sim 3$ m for elephants, which must thus generate relatively large pressures in order to counter gravitational forces that are negligible for other creatures.

3.2. *Viscous suction* $(Re(h/d) \ll 1)$

Many insects such as butterflies and mosquitoes feed on nectar or blood with their probosci. For such creatures, typically, $h \sim 1$ cm, $0.001 < \mu < 0.1$ Pa s, $u \sim 1$ cm s^{-1}, $\rho \sim 1000$ kg m^{-3} and $d \sim 100$ μm (Kingsolver & Daniel 1979; Pivnick & McNeil 1985; Lee *et al.* 2009), so that $Re(d/h) \ll 1$, indicating that inertial effects are negligible. Thus, the fluid motion is described by Poiseuille flow, for which $k_2 = 8$ in (3.2), and the flow speed is given by $u \sim d^2\Delta P/(32\mu h)$. The viscosity of nectar increases exponentially with sugar concentration; specifically, $\mu = 0.0013$ Pa s for a 10 % sugar solution and 0.06 Pa s for a 60 % solution (Weast 1974). By measuring the

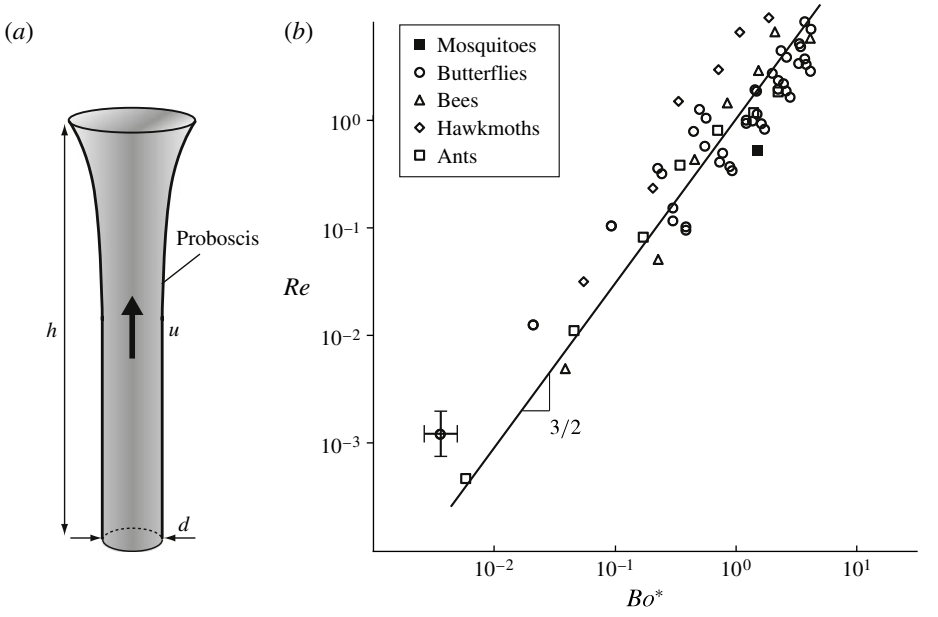

FIGURE 4. (*a*) Schematic illustration of the proboscis. (*b*) The dependence of $Re = \rho u d/\mu$ on Bo^* as defined in (3.7) for viscous suction feeders: mosquitoes (Rosenson *et al.* 1996; Lee *et al.* 2009), butterflies (May 1985; Pivnick & McNeil 1985; Boggs 1988), bees (Borrell 2006), hawkmoths (Josens & Farina 2001) and ants (Paul & Roces 2003).

dependence of flow rate on sugar concentration, Pivnick & McNeil (1985) inferred that butterflies apply constant suction power in drinking, regardless of nectar concentration. The work per unit time required to overcome the viscous friction on the wall, or equivalently the power output $\dot{W}$ of the pump, is given by $\dot{W} = Q\Delta P$, where Q is the volumetric flow rate. Expressing ΔP in terms of Q then yields

$$Re = \frac{\rho u d}{\mu} \sim \frac{\rho d^3 \dot{W}}{32\mu^2 h Q}, \tag{3.6}$$

where $\dot{W}$ depends in general on both species and individual.

The dependence of flux Q on sugar concentration s has been reported for many insects (May 1985; Pivnick & McNeil 1985; Boggs 1988; Josens & Farina 2001; Paul & Roces 2003; Borrell 2006). Kim *et al.* (2011) compiled the data, which indicate that $\mathrm{d}Q(s)/\mathrm{d}s < 0$: flux decreases with increasing sugar concentration s. Using our upper bound on applied suction pressure, $\Delta P_{max} \sim 10$ kPa, we can assess $\dot{W} \sim Q\Delta P_{max}$ for each individual creature. Eliminating d in (3.6) with $Bo = \rho g d^2/\sigma$ yields

$$\log Re \sim \frac{3}{2}\left(\log Bo + \frac{2}{3}\log\frac{\sigma^{3/2}\dot{W}}{32\mu^2 h \rho^{1/2} g^{3/2} Q}\right) \equiv \frac{3}{2}\log Bo^*. \tag{3.7}$$

We thus expect a slope of 3/2 in the plot of Re versus Bo^*, as is evident in figure 4.

Nectar drinkers have an incentive to feed quickly, specifically the threat of predation. While the sweetest nectar offers the greatest energetic rewards, it is also the most viscous and so the most difficult to transport. Kingsolver & Daniel (1979) pointed out that one might thus anticipate an optimal sugar concentration for which the energy intake rate is maximized. Since $Q \sim u$, (3.6) indicates that $Q \sim \mu^{-1/2}$ for a particular

creature, provided $\dot{W}$ is constant. The energy intake rate $\dot{E}$ is proportional to both s and Q, so $\dot{E} \sim sQ \sim s\mu^{-1/2}$. Considering the dependence of nectar viscosity $\mu(s)$ on s reported by Weast (1974), Kim *et al.* (2011) demonstrated that $\dot{E}$ is maximized with respect to s subject to the constraint of constant work rate for $s \sim 33\,\%$, which represents the optimal sugar concentration for viscous suction feeders.

3.3. *Capillary suction*

Hummingbirds, honeyeaters and sunbirds use their long tongues to collect floral nectar from the tubular corollas of flowers. The distal portion of the bird's tongue has a C-shaped groove consisting of a thin keratinized membrane, from which vascular and nervous tissues recede (Weymouth, Lasiewski & Berger 1964; Hainsworth 1973). Consequently, the bird has no muscular control over the shape of its tongue and active suction is impossible; instead, these birds rely on capillarity. When the tongue is extended out of the bill and touches the nectar, capillary pressure drives the nectar into the grooves. The tongue, once loaded with nectar, is then retracted into the bill (Rico-Guevara & Rubega 2011). While extending the tongue again in the next cycle, the hummingbird keeps the gap between its upper and lower bills smaller than the width of the tongue, thereby squeezing the nectar out of the tongue (Ewald & Williams 1982).

For creatures employing capillary suction, specifically hummingbirds and honeyeaters, typically $h \sim 1$ cm, $0.001 < \mu < 0.1$ Pa s and $u \sim hf \sim 10$ cm s^{-1}, where $f \sim 10$ Hz is the tongue insertion frequency, $\rho \sim 1000$ kg m^{-3} and $d \sim 100$ µm (Kingsolver & Daniel 1983). Therefore, $Re(d/h) < 1$, indicating negligible inertial effects, and (3.4) again reduces to Poiseuille flow,

$$\Delta P \sim \left(\frac{32}{Re(d/h)}\right)\rho u^2, \tag{3.8}$$

where now $\Delta P \sim 4\sigma/d$ and the height of the nectar is time-dependent: $h = h(t)$ and $u = h'(t)$. The solution of the force balance, $\sigma d = 8\mu h h'$, with initial condition $h(0) = 0$, is given by Washburn's law: $h(t) = (d\sigma t/4\mu)^{1/2}$. Capillary suction consists of repeated cycles of tongue insertion and retraction. Over the nectar loading time in a single cycle, T, the average flow speed is given by

$$\overline{u} \sim h(T)/T \sim (\sigma d f/(2\mu))^{1/2}. \tag{3.9}$$

The average volumetric flow rate is thus given by

$$Q \sim \frac{\pi d^2}{4}\overline{u} \sim \left(\frac{\pi^2 d^5 f}{32\mu}\right)^{1/2}, \tag{3.10}$$

where f depends only weakly on viscosity (Roberts 1995), so $Q \sim \mu^{-1/2}$. To test this proposed scaling against experimental data, Kim *et al.* (2011) introduced a relation between Q and μ, i.e. $Q = X\mu^n$, where X is a geometry-dependent prefactor that we expect to be different for each individual. If we plot Q as a function of μ on a log scale, n and X represent the slope and the offset on the y-axis, respectively. For each individual creature, we calculate an average value $\langle X\rangle = \langle Q\mu^{-n}\rangle$ based on the measured dependence of flow rate on viscosity. Figure 5(*b*) indicates the dependence of $Q/\langle X\rangle$ on μ, and that the observed dependence, $Q \sim \mu^{-1/2}$, is consistent with our expectation. We note that the dependence of Q on μ for capillary suction is the same as that for active viscous suction, so $Q \sim \mu^{-1/2}$. The optimal sugar concentration,

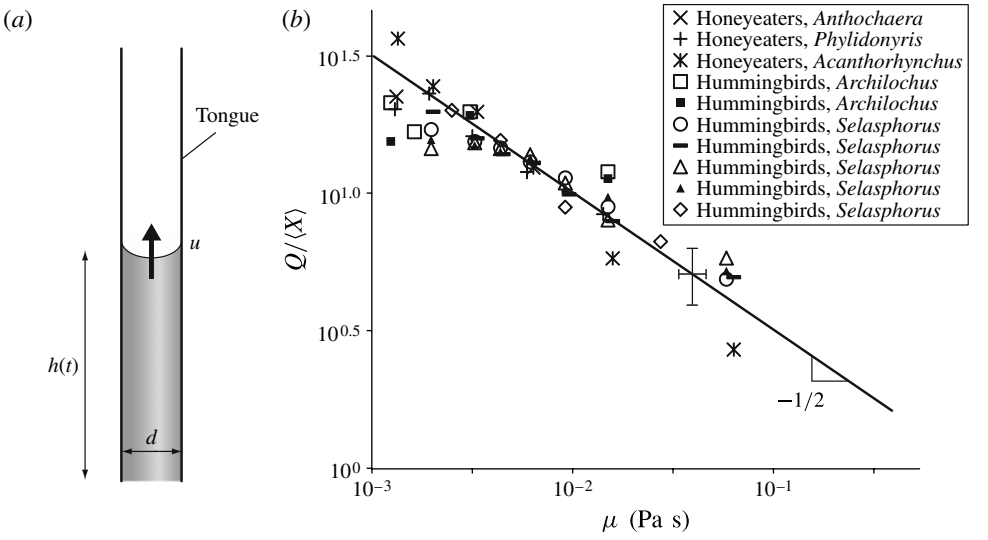

FIGURE 5. (*a*) Schematic illustration of the hummingbird's tongue. (*b*) The dependence of Q on μ for hummingbirds (Hainsworth 1973; Tamm & Gass 1986; Roberts 1995) and honeyeaters (Mitchell & Paton 1990). The line represents $Q \sim \mu^{-1/2}$, as anticipated from our scaling (3.10).

specifically that which maximizes energy flux $\dot{E} \sim sQ$, is thus 33 % for both active viscous and capillary suction (Kim *et al.* 2011).

3.4. *Capillary origami and the hummingbird's tongue*

Py *et al.* (2007) demonstrated the possibility of capillary origami, the folding of flexible solids by interfacial forces. The authors placed water drops on thin sheets with thickness δ and Young's modulus E, thus demonstrating that, provided the largest sheet dimension exceeds the elastocapillary length, $l_E = (E\delta^3/\sigma)^{1/2}$, the sheet will fold up in response to the interfacial forces. Rico-Guevara & Rubega (2011) demonstrated that the hummingbird's tongue closes around the nectar, and so is a natural example of capillary origami. Kim *et al.* (2012) further demonstrated that the tongue is a self-assembly siphon, deforming then drawing in fluid through the action of interfacial forces. Since the thickness of the hummingbird's tongue is of order 10 μm (Hainsworth 1973), $l_E \sim 1$ mm is comparable to the perimeter of the tongue, $\pi d \sim 500$ μm. One thus expects that capillary forces may deform the tongue during nectar loading, causing the initially open tongue to close. Figure 6 illustrates the rise of nectar along the hummingbird tongue, as reported in Kim *et al.* (2012). The entrained nectar passes along the deformable groove, whose shape depends on the bending stiffness and initial opening angle of the tongue. As the nectar rises, the tongue's outer diameter contracts, indicating the tongue's flexibility. Given that tongue flexure at once decreases the cross-sectional area while increasing the driving capillary pressure, one might anticipate an optimal tongue stiffness and opening angle, for which nectar intake rate is maximized.

Kim *et al.* (2012) developed a dynamic model for the hummingbird's drinking and elucidated the dependence of nectar intake rate on the tongue's flexibility and opening angle. Based on the cross-sectional shape of the distal portion of the tongue of *Selasphorus sasin* (Weymouth *et al.* 1964), the groove was modelled as an open

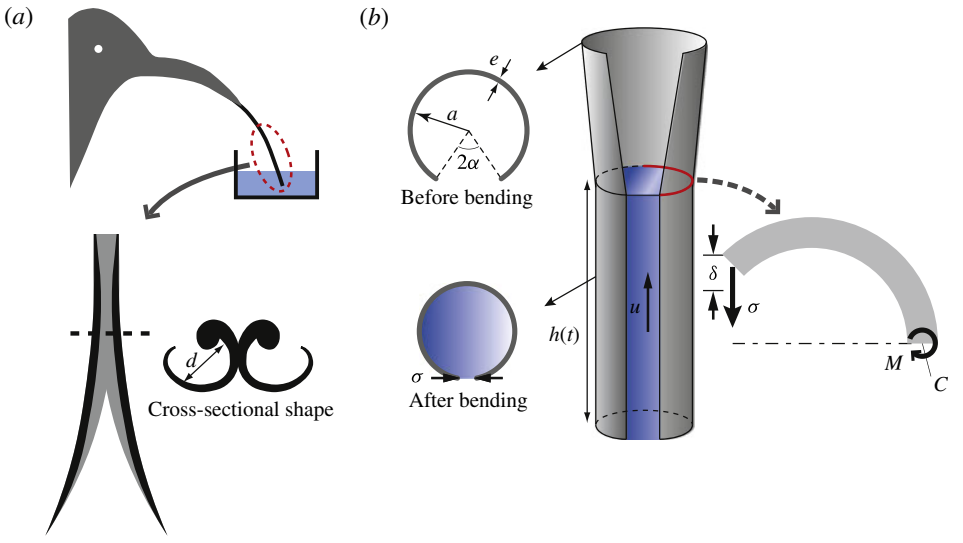

FIGURE 6. (Colour online) (*a*) Sketch of the hummingbird's tongue. (*b*) Schematic illustration of nectar rising along the hummingbird's flexible tongue, which zips up along its length in response to the surface tension of the air–water interface.

circular groove without longitudinal variation (see figure 6*b*). Gravitational effects are negligible, and the deformation of the tongue is caused principally by the surface tension acting along its lateral edges. Balancing moments about the midpoint C of the semicircle yields the bending moment per unit length at the cross-section, $M \sim \sigma a$. The displacement δ at the edge scales as $\delta \sim (M/B)a^2 \sim \sigma a^3/B$, where B is the bending stiffness per unit length. The dimensionless displacement is given by $\delta/a \sim \Gamma$, where $\Gamma = a^2\sigma/B$ represents the control parameter of the system, specifically the relative magnitudes of capillary pressures and bending stresses. By deducing the rise height $h(t)$ in terms of a, α and Γ, Kim *et al.* (2012) expressed the energy intake rate as $\dot{E} = fcAh(T)$, where f is the suction frequency, T the loading time and c the energy per volume of the nectar. The results reveal that, for a fixed Γ, the energy intake rate is maximized for an opening angle 2α of approximately 150° (see figure 6*b*). Therefore, the model provides new rationale for the fact that the hummingbird's tongue is typically semicircular in cross-section.

4. Capillary and viscous entrainment

4.1. *Viscous dipping*

We present a simple model for a nectar drinking strategy in which the fluid is entrained by the outer surface of the tongue through the combined action of viscosity and capillarity. This drinking style, henceforth 'viscous dipping' (Kim *et al.* 2011), is used by most bees, some ants and nectar-feeding bats, whose tongues are solid rather than hollow (see figure 7). Dipping is generally characterized by an extensible tongue being immersed into nectar, coated, then extracted in a cyclic fashion. For bees, the tongue diameter d and length h are typically of order 200 μm and 2 mm, respectively, and the tongue extraction speed $u \sim 2$ cm s^{-1}. We expect the volume entrained to be proportional to the area of the immersed tongue surface and the thickness e of the nectar layer. The average volumetric flow rate must thus scale as $Q \sim \pi deu$, where u is

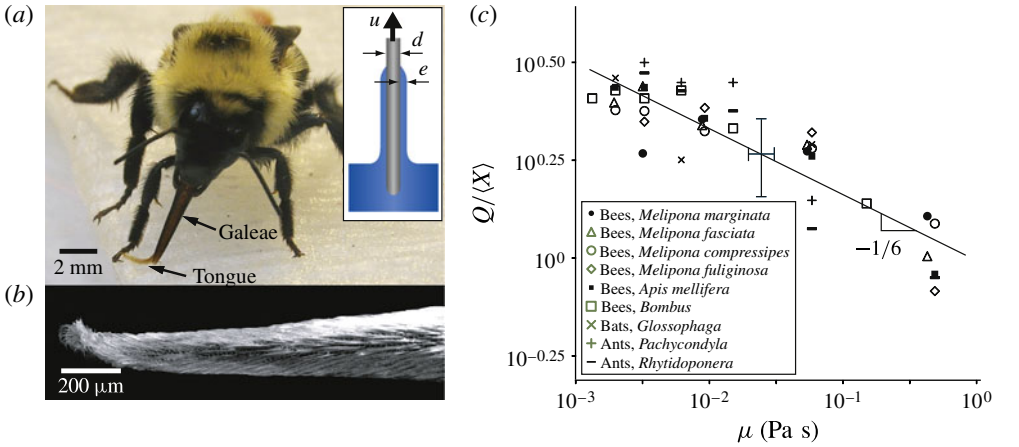

FIGURE 7. (Colour online) (*a*) A bumblebee drinking. Inset: schematic illustration of the bee's tongue. (*b*) Scanning electron microscope image of the bumblebee's tongue. (*c*) The dependence of Q on μ for bats (Roces *et al.* 1993), bees (Roubik & Buchmann 1984; Harder 1986) and ants (Paul & Roces 2003), all of which employ viscous dipping. The line corresponds to the scaling suggested by (4.1), specifically, $Q \sim \mu^{-1/6}$.

tongue speed. For steady flows, Landau–Levich–Derjaguin theory predicts $e \sim dCa^{2/3}$ in the limit of $Ca < 0.1$, $We \ll 1$ and $Bo \ll 1$, where $We = \rho u^2 d/\sigma$ is the Weber number, $Ca = \mu u/\sigma$ and $Bo = \rho g d^2/\sigma$ (Quéré 1999). Kim *et al.* (2011) introduced the assumption that the work rate applied in dipping is independent of μ for a given creature. The retraction of the tongue through the viscous nectar requires the power $\dot{W} \sim \mu h u^2$ to overcome the viscous drag. Expressing the volume intake rate in terms of $\dot{W}$ yields

$$Q \sim \pi d e u \sim \frac{\pi d^2 \dot{W}^{5/6}}{\sigma^{2/3} h^{5/6} \mu^{1/6}}, \tag{4.1}$$

so $Q \sim \mu^{-1/6}$ for each individual creature. For the relation between Q and μ, $Q = X\mu^n$ (as introduced in § 3.3), we estimate an average value $\langle X\rangle = \langle Q\mu^{-n}\rangle$ based on the measured dependence of flow rate on viscosity (Roubik & Buchmann 1984; Harder 1986; Roces *et al.* 1993; Paul & Roces 2003). Figure 7 illustrates the dependence of $Q/\langle X\rangle$ on μ, and indicates that the observed dependence of Q on μ, specifically $Q \sim \mu^{-1/6}$, is consistent with our prediction (4.1). Using this scaling $Q \sim \mu^{-1/6}$, Kim *et al.* (2011) inferred that the energy intake rate $\dot{E} \sim sQ \sim s\mu^{-1/6}$ is maximized subject to the constraint of constant work rate for $s \sim 52\,\%$, which roughly corresponds to the measured optimal sugar concentrations for creatures that drink via viscous dipping. The model provides new rationale for why the measured optimal concentrations are higher for creatures that use viscous dipping (50–60 %) than for creatures that use suction (30–40 %).

4.2. *Licking*

Lizards and rats lick water, a process relying on multiple cycles of tongue immersion and retraction. While licking resembles dipping in nectar feeders such as bees and ants in some regards, the licking mechanism is qualitatively different. We note that, for dipping in nectar feeders, the high viscosity of nectar results in a thick layer of nectar

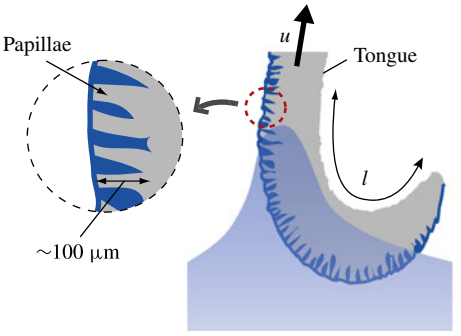

FIGURE 8. (Colour online) Schematic illustration of licking, the drinking strategy common to lizards and rats. Fluid imbibition into the papillae plays a critical role in increasing the volume entrained.

on the tongue, and a relatively large volume of nectar transported to the mouth. For the lizard, the tongue speed for licking $u \sim 1$ cm s^{-1}, so $Ca = u\mu/\sigma \sim 10^{-4}$, while the tongue width $w \sim 4$ mm and extrusion length $l \sim 2$ mm are comparable to the capillary length l_c (Wagemans *et al.* 1999). Thus Landau–Levich–Derjaguin theory predicts that the film thickness of the water layer on the tongue is given by $e \sim l_c Ca^{2/3} \sim 10$ μm (Quéré 1999). The water intake rate should thus be given by $Q \sim el^2 f \sim 0.5$ μl s^{-1}, where $f \sim 3$ Hz is the observed licking frequency. However, measurements of volume uptake in rats of $Q \sim 10$ μl s^{-1} suggest the importance of a physiological adaptation, specifically the papillae on the tongue. Rabinowitz & Tandler (1986) reported that the tongue of the chameleon has papillae whose depth is of order 100 μm. Since this depth is significantly greater than the coating thickness of water on the tongue, the efficiency of this licking mechanism is evidently greatly enhanced by the capillary imbibition of water into the papillae (see figure 8). Fluid is expelled from the papillae during the final phase of licking, when the tongue is straightened and contracted. Based on the similar tongue sizes and drinking behaviour of rats, we suspect that they employ a similar drinking strategy.

5. Inertial entrainment: lapping and ladling

Owing to the open geometry of their cheeks, many creatures in the biological family *Felidae* (e.g. house cats and lions) and *Canis* (e.g. dogs and wolves) cannot seal their mouths in order to generate suction; consequently, they drink by moving their tongue in a lapping motion. These creatures extend their tongues to the water, curled ventrally into a ladle shape. After contacting the water, the tongue is retracted, transporting entrained water with it. When the tongue is retracted to a height H, the creatures catch the entrained water by closing their jaws at some intermediate height (see figure 9*a*,*b*). With the characteristic half-width of the tongue tip $R \sim 1$ cm and tongue speed $u > 10$ cm s^{-1}, $Re = \rho uR/\mu > 1000$ and $Bo = \rho gR^2/\sigma \sim 10$, indicating negligible viscous effects and capillary pressures. For this class of creatures, the water is thus raised mouthwards through inertial entrainment.

Reis *et al.* (2010) elucidated the drinking technique of cats, using high-speed videography, which indicates that cats do not immerse the tongue in water, so water is entrained only below the tongue. From analog laboratory experiments, they

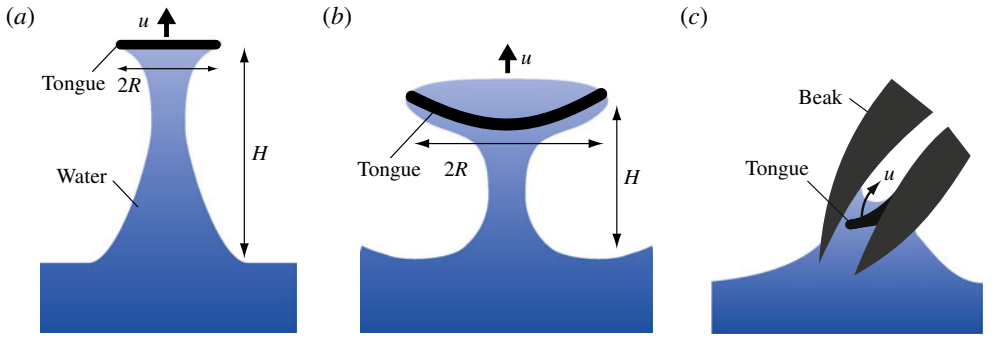

FIGURE 9. (Colour online) Schematic illustration of ladling by (*a*) cats, (*b*) dogs and (*c*) zebra finches (Heidweiller & Zweers 1990).

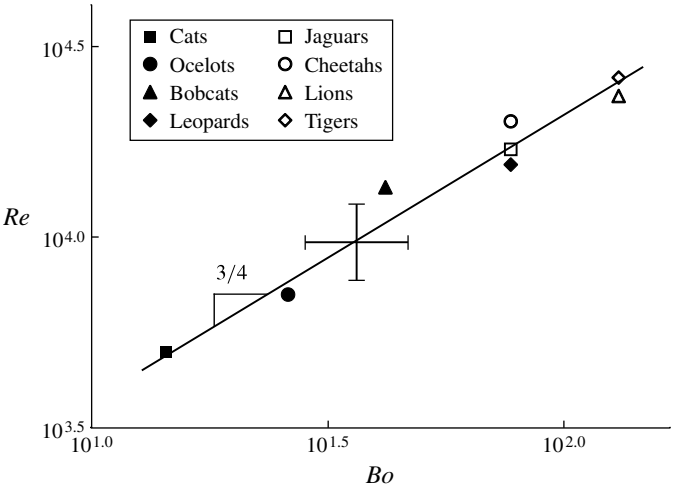

FIGURE 10. The dependence of $Re = \rho uR/\mu$ on $Bo = \rho gR^2/\sigma$ for lapping cats. Data of u and R (Reis *et al.* 2010) were estimated from f and M with the assumption of body shape isometry in *Felidae*.

demonstrated that the entrained water volume, specifically that displaced above the initially horizontal interface, increases up to order R^3 shortly before pinch-off and then sharply decreases. They observed that the cat catches the raised water just before pinch-off and thus ingests a water volume of order R^3. The study further demonstrates that the lapping frequency f is that which maximizes the volume flux of water, i.e. $f \sim (gH)^{1/2}/R$. The assumption of isometry suggests that H and R will be proportional to body size, so that the lapping frequency is $f \sim \ell^{-1/2}$, where ℓ is the characteristic body size. Therefore, the tongue velocity $u \sim Rf \sim \ell^{1/2}$ and $Re = \rho uR/\mu \sim \ell^{3/2}$. Since $Bo = \rho gR^2/\sigma \sim \ell^2$, we expect $Re \sim Bo^{3/4}$. Isometry of *Felidae* would indicate that the tongue width scales as $R \sim M^{1/3}$ (McMahon & Bonner 1983), where M is the body weight, and that the tongue speed scales as $u \sim fR \sim fM^{1/3}$. From the data on M and f for various felines (Reis *et al.* 2010), we plot the dependence of Re on Bo in figure 10. Here, the slope is consistent with our expectation, specifically $Re \sim Bo^{3/4}$.

Using X-ray videography, Crompton & Musinsky (2011) recently examined the drinking technique of dogs. They demonstrated that, as for the cat, fluid is entrained onto the base on the tongue; however, it is also entrained above the tongue. Their high-speed videos indicate that the dog immerses its tongue into the water before extracting it, thereby entraining fluid both above and below the tongue. Since the dog also closes its jaws before the entrained water column pinches off, the volume entrained below the tongue is of order R^3, as for the cat. The ladling tongue may be roughly described as a bowl of radius R, so the dog can ingest volumes of order R^3 entrained both above and below the tongue.

The delineation between the various drinking strategies is never entirely clear. Zebra finches use a variant of ladling that depends explicitly on capillary pressure, as one might anticipate since the tongue size $R \sim 1$ mm and $Bo \sim 1$. The zebra finch immerses its beak into the water surface with a slight opening angle, causing water to rise by capillary action into the resulting gap (see figure 9*c*). It then ladles water with its tongue in order to transport water to the oesophagus. This drinking style is markedly different from that of many other birds, such as pigeons, which suck water into their mouths by closing their beaks and applying suction across the resulting thin gap. We note that birds, for which characteristic tongue and beak sizes are often comparable to the capillary length $l_c = (\sigma/\rho g)^{1/2} \sim 2$ mm, may generally use either suction or capillary pressure. Indeed, drinking strategies in birds often depend on the interplay of these two forces.

6. Contact angle hysteresis

The equilibrium contact angle θ_e of a drop on a solid is prescribed by Young's law, $\sigma \cos\theta_e = \gamma_{SG} - \gamma_{SL}$, where γ_{SG} and γ_{SL} are the interfacial energies per unit area between solid–gas and solid–liquid, respectively. In reality, for a given solid–fluid combination, a range of static contact angles may arise (Dettre & Johnson 1964). Consider a drop of fluid emplaced on a solid. If the drop is filled, it will grow, and its contact angle will increase progressively until it reaches a critical value, θ_a, at which the contact line begins to advance. If, conversely, fluid is withdrawn from the drop, its contact angle will decrease progressively until it reaches a critical value, θ_r, at which the contact line begins to recede. The observed static contact angles θ may thus lie anywhere within the range $\theta_r < \theta < \theta_a$, bounded below and above by the receding and advancing contact angles. While contact angle hysteresis normally impedes drop motion along surfaces, several creatures have evolved unique drinking strategies that exploit it.

The Namib beetle resides in a desert where it rarely rains; nevertheless, it is able to condense water from micrometre-scale fog droplets that sweep in daily from the coast. Their surface is composed of hydrophilic bumps on hydrophobic valleys. The fog droplets thus stick to the peaks, remaining pinned there by contact angle hysteresis, then grow through accretion until becoming large enough to be blown by the wind onto the hydrophobic valleys, across which they roll with little resistance (see figure 11*a*). By guiding these rolling droplets towards their mouths, the beetles reap the rewards of the refrigeration-free condenser on their backs (Parker & Lawrence 2001).

Phalaropes are small birds that inhabit the American and Russian coastlines of the Arctic seas and prey on small aquatic organisms such as miniature shrimp and phytoplankton. By swimming in a tight circle on the surface of shallow bodies of water, they generate a vortex that sweeps their prey upwards, like tea leaves in a

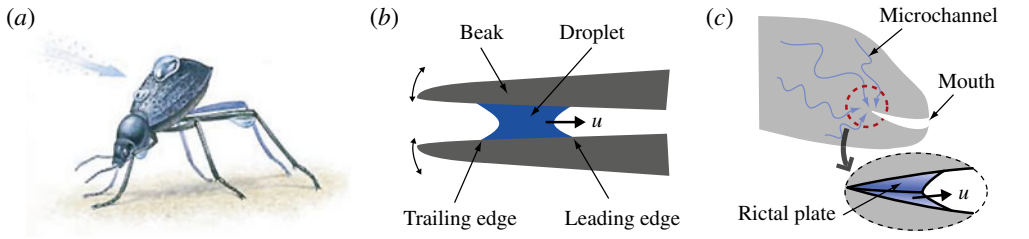

FIGURE 11. (Colour online) Schematic illustrations of the drinking strategies of (*a*) the Namib desert beetle (image courtesy of Roberto Osti Illustrations), (*b*) the Phalarope and (*c*) the Texas horned lizard, all of which rely critically on contact angle hysteresis.

swirling cup (Rubega & Obst 1993). By pecking the free surface, they capture a prey-bearing droplet in the tip of their beak. Then, by successively opening and closing their beaks in a tweezering motion, they draw the droplet mouthwards. Prakash *et al.* (2008) demonstrated that this capillary ratchet mechanism relies critically on contact angle hysteresis. During the closing phase of the tweezering motion, both contact lines of the droplet have the tendency to progress outwards, but the leading edge always does so first while the trailing edge is pinned due to the contact angle hysteresis (see figure 11*b*). Conversely, during the opening phase, both contact lines tend to retreat inwards, but the trailing edge does so first. The drop thus advances through a ratcheting motion. In each cycle, both leading and trailing edges of the contact lines advance and retreat; however, owing to the asymmetry in the wedge geometry, net mouthward drop motion is achieved. This drinking strategy illustrates how contact angle hysteresis may, when coupled to dynamic boundary motion, enhance rather than impede drop transport.

Some lizards such as Australian thorny devils and Texas horned lizards, live in environments where water is rarely encountered in the form of extended bodies of water such as puddles or ponds. The lizards have thus evolved a novel rain-harvesting technique that relies on their integumental morphology. The skin of the lizard consists of multiple layers whose warped shape forms microchannels that uptake water from any source, from raindrops to wet soils, via capillary action (Sherbrooke *et al.* 2007). The water is transported through the skin to the base of the mouth through the microchannels; however, it has not yet been clearly elucidated how the lizard uptakes the water from the microchannels. Specifically, once the capillary network of its skin is filled with water, capillarity suction can no longer play a role; therefore, the lizard requires a pumping system (Sherbrooke 2004). The lizard has a rictal plate, a fold of skin at the corner of the mouth whose geometry is controlled by the jaw movement (see figure 11*c*). Sherbrooke (2004) proposed that the jaw movement may draw water into the mouth through contact angle hysteresis, in a manner reminiscent of the phalarope. Further study is under way to elucidate this subtle drinking mechanism.

7. Discussion

Nature's myriad drinking techniques make clear that the optimal fluid transport mechanism for a given creature depends on both its geometry and its scale. We have identified the dominant forces and suggested physical pictures for each drinking style, thereby classifying the natural drinking styles of terrestrial creatures according to mechanism. Simple scaling arguments have been validated by comparison with

existing data. Suction is the most common drinking strategy, the suction pressure being applied to overcome either viscous forces for small creatures ($Re < 1$) or inertial forces for large creatures ($Re > 1$). In suction, gravitational effects are negligible for all but the largest creatures. Since the pressure generated by muscular contraction is comparable for all creatures, we deduced that the pressure generated by muscular contraction is typically larger than the characteristic capillary pressure. Nevertheless, capillary pressure is employed by some small creatures and others for which morphological constraints preclude active suction. Creatures for which suction is impossible have developed various drinking styles. Inertial forces facilitate lapping or ladling for large creatures ($Bo > 1$), while interfacial and viscous forces facilitate licking and viscous dipping for small creatures. A few such small creatures have developed ingenious drinking techniques that rely critically on contact angle hysteresis. The critical importance of wetting properties in the drinking strategies of these creatures makes immediately clear their vulnerability to surface-active pollutants such as petroleum or detergent.

Guided by the presupposition that evolution leads to optimal design, it is natural for mathematicians to attempt to rationalize natural systems through consideration of constrained optimization problems. However, it is rarely clear what, precisely, is being optimized and what are the relevant constraints. For example, attempting to rationalize the shapes of bird beaks or insect probosci exclusively in terms of their drinking efficiency would mistakenly neglect their importance in many other tasks, for example, foraging and combat. Nevertheless, we have considered a number of instances where it is fruitful to consider the role of optimization in natural drinking strategies. In particular, we have demonstrated that the optimal sugar concentrations for nectar feeding via viscous dipping or active suction can be rationalized as those that maximize energy flux subject to the constraint of constant work rate (Kim *et al.* 2011).

Nature has been optimizing drinking strategies among small creatures for millions of years while humans have only recently become interested in transporting fluid on the nanolitre scale, for applications ranging from drug delivery to the handling of biomolecules (Stone, Stroock & Ajdari 2004). Although biomimicry is now a central scientific theme, nature's myriad mechanisms for fluid transport on the scale of interest to microfluidics remain relatively unexplored. It seems likely that natural drinking techniques may inspire and inform fluid transport mechanisms for microfluidic technologies. For example, Zhai *et al.* (2006) demonstrated that 'Super Plastic', the manufactured surface that mimics the Namib beetle's back, can be applied to water harvesting in the developing world; and Garrod *et al.* (2007) investigated the optimal surface topology for maximizing the water harvesting rate. Bush *et al.* (2010) discussed the application of the phalarope's drinking mechanism to digital microfluidic transport, an application that would benefit from the biomimetic unidirectional surfaces explored by Prakash & Bush (2011). It is hoped that continued exploration of this class of problem will prompt further biomimetic technological advance.

Acknowledgements

The authors thank NSF and the STX Scholarship Foundation for financial support. We gratefully acknowledge T. Gilet for many valuable discussions, and F. Peaudecerf and M. Baldwin for their contributions to our understanding of the hummingbird's drinking technique.

REFERENCES

ADOLPH, E. F. 1939 Measurements of water drinking in dogs. *Am. J. Physiol.* **125**, 75–86.

ANDERSSON, M., SCHAAR, J. & WIKTORSSON, H. 1984 Effects of drinking water flow rates and social rank on performance and drinking behaviour of tied-up dairy cows. *Livest. Prod. Sci.* **11**, 599–610.

BELS, V. L., DAVENPORT, J. & RENOUS, S. 1995 Drinking and water expulsion in the diamondback turtle *Malaclemys terrapin*. *J. Zool.* **236**, 483–497.

BENNET-CLARK, H. C. 1963 Negative pressures produced in the pharyngeal pump of the blood sucking bug, *Rhodnius prolixus*. *J. Expl Biol.* **40**, 223–229.

BENTLEY, P. J., BRETZ, W. L. & SCHMIDT-NIELSEN, K. 1967 Osmoregulation in the diamondback terrapin, *Malaclemys terrapin centrata*. *J. Expl Biol.* **46**, 161–167.

BERKHOUDT, G., KARDONG, K. V. & ZWEERS, G. A. 1995 Mechanics of drinking in the brown tree snake, *Boiga irregularis*. *Zoology* **98**, 92–103.

BOGGS, C. L. 1988 Rates of nectar feeding in butterflies: effects of sex, size, age and nectar concentration. *Funct. Ecol.* **2**, 289–295.

BORRELL, B. J. 2006 Mechanics of nectar feeding in the orchid bee *Euglossa imperialis*: pressure, viscosity and flow. *J. Expl Biol.* **209**, 4901–4907.

BORRELL, B. J. 2007 Scaling of nectar foraging in orchid bees. *Am. Nat.* **169**, 569–580.

BOTT, E., DENTON, D. A. & WELLER, S. 1965 Water drinking in sheep with oesophageal fistulae. *J. Physiol.* **76**, 323–336.

BUSH, J. W. M. & HU, D. L. 2006 Walking on water: biolocomotion at the interface. *Annu. Rev. Fluid Mech.* **38**, 339–369.

BUSH, J. W. M., HU, D. L. & PRAKASH, M. 2008 The integument of water-walking arthropods: form and function. *Adv. Insect Physiol.* **34**, 117–192.

BUSH, J. W. M., PEAUDECERF, F., PRAKASH, M. & QUÉRÉ, D. 2010 On a tweezer for droplets. *Adv. Colloid Interface Sci.* **161**, 10–14.

CARPENTER, P. W., BERKOUK, K. & LUCEY, A. D. 2003 Pressure wave propagation in fluid-filled co-axial elastic tubes. Part 2. Mechanisms for the pathogenesis of syringomyelia. *Trans. ASME: J. Biomech. Engng* **125**, 857–863.

CARRÉ, A. & MITTAL, K. L. 2009 *Superhydrophobic Surfaces*. VSP/Brill.

CROMPTON, A. W. & MUSINSKY, C. 2011 How dogs lap: ingestion and intraoral transport in *Canis familiaris*. *Biol. Lett.* **7**, 882–884.

CUNDALL, D. 2000 Drinking in snakes: kinematic cycling and water transport. *J. Expl Biol.* **203**, 2171–2185.

DANIEL, T. L. & KINGSOLVER, J. G. 1983 Feeding strategy and the mechanics of blood sucking in insects. *J. Theor. Biol.* **105**, 661–672.

DAVENPORT, J. & MACEDO, E.-A. 1990 Behavioural osmotic control in the euryhaline diamondback terrapin *Malaclemys terrapin*: responses to low salinity and rainfall. *J. Zool.* **220**, 487–496.

DETTRE, R. H. & JOHNSON, R. E. 1964 Contact angle hysteresis II. Contact angle measurements on rough surfaces. In *Contact Angle, Wettability, and Adhesion* (ed. F. M. Fowkes). *Advances in Chemistry Series*, vol. 43, pp. 136–144. American Chemical Society.

EWALD, P. W. & WILLIAMS, W. A. 1982 Function of the bill and tongue in nectar uptake by hummingbirds. *The Auk* **99**, 573–576.

GARROD, R. P., HARRIS, L. G., SCHOFIELD, W. C. E., MCGETTRICK, J., WARD, L. J., TEARE, D. O. H. & BADYAL, J. P. S. 2007 Mimicking a Stenocara beetle's back for microcondensation using plasmachemical patterned superhydrophobic–superhydrophilic surfaces. *Langmuir* **23**, 689–693.

GILLIS, G. B. & LAUDER, G. V. 1994 Aquatic prey transport and the comparative kinematics of *Ambystoma tigrinum* feeding behaviours. *J. Expl Biol.* **187**, 159–179.

GROTBERG, J. B. 1994 Pulmonary flow and transport phenomena. *Annu. Rev. Fluid Mech.* **26**, 529–571.

HAINSWORTH, F. R. 1973 On the tongue of a hummingbird: its role in the rate and energetics of feeding. *Compar. Biochem. Phys.* **46A**, 65–78.

HARDER, L. D. 1986 Effects of nectar concentration and flower depth on flower handling efficiency of bumble bees. *Oecologia* **69**, 309–315.

HEIDWEILLER, J., VAN LOON, J. A. & ZWEERS, G. A. 1992 Flexibility of the drinking mechanism in adult chickens (*Gallus gallus*) (Aves). *Zoomorphology* **111**, 141–159.

HEIDWEILLER, J. & ZWEERS, G. A. 1990 Drinking mechanisms in the zebra finch and the bengalese finch. *The Condor* **92**, 1–28.

JOSENS, R. B. & FARINA, W. M 2001 Nectar feeding by the hovering hawk moth *Macroglossum stellatarum*: intake rate as a function of viscosity and concentration of sucrose solutions. *J. Compar. Physiol.* **187**, 661–665.

KIM, W., GILET, T. & BUSH, J. W. M. 2011 Optimal concentrations in nectar feeding. *Proc. Natl Acad. Sci. USA* **108**, 16 618–16 621.

KIM, W., PEAUDECERF, F., BALDWIN, M. & BUSH, J. W. M. 2012 The hummingbird's tongue: a self-assembling capillary syphon. *Proc. Roy. Soc.* B (submitted).

KINGSOLVER, J. G. & DANIEL, T. L. 1979 On the mechanics and energetics of nectar feeding in butterflies. *J. Theor. Biol.* **76**, 167–179.

KINGSOLVER, J. G. & DANIEL, T. L. 1983 Mechanical determinants of nectar feeding strategy in hummingbirds: energetics, tongue morphology, and licking behaviour. *Oecologia* **60**, 214–226.

KOOLOOS, J. G. M. & ZWEERS, G. A. 1989 Mechanics of drinking in the mallard (*Anas platyrhynchos*, Anatidae). *J. Morphol.* **199**, 327–347.

LAUGA, E. & POWERS, T. R. 2009 The hydrodynamics of swimming microorganisms. *Rep. Prog. Phys.* **72**, 096601.

LEE, S. J., KIM, B. H. & LEE, J. Y. 2009 Experimental study on the fluid mechanics of blood sucking in the proboscis of a female mosquito. *J. Biomech.* **42**, 857–864.

LIGHTHILL, M. J. 1975 *Mathematical Biofluiddynamics*. SIAM.

MADDISON, S., WOD, R. J., ROLLS, E. T., ROLLS, B. J. & GIBBS, J. 1980 Drinking in the rhesus monkeys: peripheral factors. *J. Compar. Physiol. Psychol.* **94**, 365–374.

MAY, P. G. 1985 Nectar uptake rates and optimal nectar concentrations of two butterfly species. *Oecologia* **66**, 381–386.

MCCLUNG, J. R. & GOLDBERG, S. J. 2000 Functional anatomy of the hypoglossal innervated muscles of the rat tongue: a model for elongation and protrusion of the mammalian tongue. *Anat. Rec.* **260**, 378–386.

MCMAHON, T. A. & BONNER, J. T. 1983 *On Size and Life*. Scientific American Library.

MITCHELL, R. J. & PATON, D. C. 1990 Effects of nectar volume and concentration on sugar intake rates of Australian honeyeaters (Meliphagidae). *Oecologia* **83**, 238–246.

MORRISON, N. J., RICHARDSON, J., DUNN, L. & PARDY, R. L. 1989 Respiratory muscle performance in normal elderly subjects and patients with COPD. *Chest* **95**, 90–94.

PARKER, A. R. & LAWRENCE, C. R. 2001 Water capture by a desert beetle. *Nature* **414**, 33–34.

PAUL, J. & ROCES, F. 2003 Fluid intake rates in ants correlate with their feeding habits. *J. Insect Physiol.* **49**, 347–357.

PEDLEY, T. J. 1977 Pulmonary fluid dynamics. *Annu. Rev. Fluid Mech.* **9**, 229–274.

PEDLEY, T. J. & KESSLER, J. O. 1992 Hydrodynamic phenomena in suspensions of swimming microoganisms. *Annu. Rev. Fluid Mech.* **24**, 313–358.

PIVNICK, K. A. & MCNEIL, J. N. 1985 Effects of nectar concentration on butterfly feeding: measured feeding rates for *Thymelicus lineola* (Lepidoptera: Hesperiidae) and a general feeding model for adult Lepidoptera. *Oecologia* **66**, 226–237.

PRAKASH, M. & BUSH, J. W. M. 2011 Interfacial propulsion by directional adhesion. *Intl J. Non-Linear Mech.* **46**, 607–615.

PRAKASH, M., QUÉRÉ, D. & BUSH, J. W. M. 2008 Surface tension transport of prey by feeding shorebirds: the capillary ratchet. *Science* **320**, 931–934.

PY, C., REVERDY, P., DOPPLER, L., BICO, J., ROMAN, B. & BAROUD, C. N. 2007 Capillary origami: spontaneous wrapping of a droplet with an elastic sheet. *Phys. Rev. Lett.* **98**, 156103.

QUÉRÉ, D. 1999 Fluid coating on a fibre. *Annu. Rev. Fluid Mech.* **31**, 347–384.

RABINOWITZ, T. & TANDLER, B. 1986 Papillary morphology of the tongue of the American chameleon: *Anolis carolinensis*. *Anat. Rec.* **216**, 483–489.

REIS, P. M., JUNG, S., ARISTOFF, J. M. & STOCKER, R. 2010 How cats lap: water uptake by *Felis catus*. *Science* **330**, 1231–1234.

RICO-GUEVARA, A. & RUBEGA, M. A. 2011 The hummingbird tongue is a fluid trap, not a capillary tube. *Proc. Natl Acad. Sci. USA* **108**, 9356–9360.

ROBERTS, W. M. 1995 Hummingbird licking behaviour and the energetics of nectar feeding. *The Auk* **112**, 456–463.

ROCES, F., WINTER, Y. & VON HELVERSEN, O. 1993 Nectar concentration preference and water balance in a flower visiting bat, *Glossophaga soricina antillarum*. In *Animal–Plant Interactions in Tropical Environments* (ed. W. Barthlott), pp. 159–165. Museum Koenig.

ROSENSON, R. S., MCCORMICK, A. & URETZ, E. F. 1996 Distribution of blood viscosity values and biochemical correlates in healthy adults. *Clin. Chem.* **42**, 1189–1195.

ROUBIK, D. W. & BUCHMANN, S. L. 1984 Nectar selection by melipona and *Apis mellifera* (Hymenoptera: Apidae) and the ecology of nectar intake by bee colonies in a tropical forest. *Oecologia* **61**, 1–10.

RUBEGA, M. A. & OBST, B. S. 1993 Surface-tension feeding in phalaropes: discovery of a novel feeding mechanism. *The Auk* **110**, 169–178.

SCHLAMOWITZ, R., HAINSWORTH, F. R. & WOLF, L. L. 1976 On the tongues of sunbirds. *The Condor* **78**, 104–107.

SCHMIDT-NIELSEN, B., SCHMIDT-NIELSEN, K., HOUPT, T. R. & JARNUM, S. A. 1956 Water balance of the camel. *Am. J. Physiol.* **185**, 185–194.

SHERBROOKE, W. C. 2004 Integumental water movement and rate of water ingestion during rain harvesting in the Texas horned lizard, *Phrynosoma cornutum*. *Amphibia–Reptilia* **25**, 29–39.

SHERBROOKE, W. C., SCARDINO, A. J., DE NYS, R. & SCHWARZKOPF, L. 2007 Functional morphology of scale hinges used to transport water: convergent drinking adaptations in desert lizards (*Moloch horridus* and *Phrynosoma cornutum*). *Zoomorphology* **126**, 89–102.

STONE, H. A., STROOCK, A. D. & AJDARI, A. 2004 Engineering flows in small devices: microfluidics toward a lab-on-a-chip. *Annu. Rev. Fluid Mech.* **36**, 381–411.

TAMM, S. & GASS, C. L. 1986 Energy intake rates and nectar concentration preferences by hummingbirds. *Oecologia* **70**, 20–23.

TRIANTAFYLLOU, M. S., TRIANTAFYLLOU, G. S. & YUE, D. K. P. 2000 Hydrodynamics of fishlike swimming. *Annu. Rev. Fluid Mech.* **32**, 33–53.

WAGEMANS, F., CHARDON, M., GASC, J. P., RENOUS, S. & BELS, V. L. 1999 Drinking behaviour in *Anolis carolinensis* (Voigt, 1837) and *Oplurus cuvieri* (Gray, 1831) (Reptilia: Iguania: Iguanidae). *Can. J. Zool.* **77**, 1136–1146.

WANG, Z. J. 2005 Dissecting insect flight. *Annu. Rev. Fluid Mech.* **37**, 183–210.

WEAST, R. C. 1974 *Handbook of Chemistry and Physics*. CRC Press.

WEIJNEN, J. A. 1998 Licking behaviour in the rat: measurement and situational control of licking frequency. *Neurosci. Biobehav. Rev.* **22**, 751–760.

WEST, J. B. 2001 Snorkel breathing in the elephant explains the unique anatomy of its pleura. *Respir. Physiol.* **126**, 1–8.

WEYMOUTH, R. D., LASIEWSKI, R. C. & BERGER, A. J. 1964 The tongue apparatus in hummingbirds. *Acta Anat.* **58**, 252–270.

WILSON, J. F., MAHAJAN, U., WAINWRIGHT, S. A. & CRONER, L. J. 1991 A continuum model of elephant trunks. *Trans. ASME: J. Biomech. Engng* **113**, 79–84.

WINTER, Y. & VON HELVERSEN, O. 2003 Operational tongue length in phyllostomid nectar-feeding bats. *J. Mammal.* **84**, 886–896.

WU, T. Y. 2011 Fish swimming and bird/insect flight. *Annu. Rev. Fluid Mech.* **43**, 25–58.

ZHAI, L., BERG, M. C., CEBECI, F. C., KIM, Y., MILWID, J. M., RUBNER, M. F. & COHEN, R. E. 2006 Patterned superhydrophobic surfaces: toward a synthetic mimic of the Namib desert beetle. *Nano Lett.* **6**, 1213–1217.

ZWEERS, G., DE JONG, F., BERKHOUDT, H. & BERGE, J. C. V. 1995 Filter feeding in flamingos (*Phoenicopterus ruber*). *The Condor* **97**, 297–324.

ZWEERS, G. A. 1982 Drinking of the pigeon (*Columba livia* L.). *Behaviour* **80**, 274–317.